

# Thermal Degradation Behaviors of Phosphorus–Silicon Synergistic Flame-Retardant Copolyester

Jun Li,<sup>1</sup> Hongfang Zhu,<sup>1</sup> Juan Li,<sup>1</sup> Xinyu Fan,<sup>1</sup> Xingyou Tian<sup>2</sup>

<sup>1</sup>Ningbo Key Lab of Polymer Materials, Ningbo Institute of Materials Technology and Engineering, Chinese Academy of Sciences, Ningbo, Zhejiang 315201, People's Republic of China

<sup>2</sup>Institute of Solid State Physics, Chinese Academy of Sciences, Hefei, Anhui 230031, People's Republic of China

Received 17 June 2009; accepted 29 December 2010

DOI 10.1002/app.34127

Published online 13 June 2011 in Wiley Online Library (wileyonlinelibrary.com).

**ABSTRACT:** A novel phosphorus-containing poly (ethylene terephthalate) (PET) copolyester/nano-SiO<sub>2</sub> composite (PET-co-DDP/SiO<sub>2</sub>) was synthesized by *in situ* polycondensation of terephthalic acid (TPA), ethylene glycol (EG), [(6-oxide-6H-dibenz[c,e] [1,2]oxaphosphorin-6-yl)-methyl]-butanedioic acid (DDP), and nano-SiO<sub>2</sub>. The morphology of PET nanocomposites was observed by using transmission electron microscope and scanning electron microscope. It was found that the SiO<sub>2</sub> nanoparticles were dispersed uniformly at nanoscale in the copolyesters with content 2 wt %. The thermal degradation behavior of PET nanocomposites was investigated by thermogravimetric analysis performed with air and nitrogen ambience. The activation energies of thermal degradation were determined using Kissinger and Flynn–Wall–Ozawa methods, respectively. The results obtained from Kissinger method

showed that the activation energy was increased with the introduction of SiO<sub>2</sub>. Moreover, the activation energy is decreased for PET-co-DDP system in nitrogen and air. The results also indicated that the SiO<sub>2</sub> and DDP had synergic effect on the early decomposition and the late charring in air. Furthermore, in the PET-co-DDP/SiO<sub>2</sub> system, the activation energy increased when the DDP component increased. However, the opposite results were obtained when the Flynn–Wall–Ozawa method was used. That was because the Doyle approximation stands correct as the conversion degree is from 5% to 20%. The effects of SiO<sub>2</sub> and DDP on the PET thermal degradation were lower in nitrogen than in air. © 2011 Wiley Periodicals, Inc. *J Appl Polym Sci* 122: 1993–2003, 2011

**Key words:** copolyester; degradation; synergism; kinetics

## INTRODUCTION

Poly(ethylene terephthalate) (PET) is widely used to produce fibers, films, and beverage containers because of its excellent properties, such as chemical resistance, high mechanical strength, melt mobility, and spinnability. However, like other polymer materials, flammability of PET dramatically limits their applications in many fields. Much attention has been addressed on the research of flame-retardant PET, which incorporates reactive phosphorus-containing monomers into the polymer chains. Some phosphorus-containing flame retardants (PCFRs) and copolyesters have been synthesized, and their properties were investigated and reported in literatures.<sup>1–5</sup> However, it is difficult to obtain polymer materials with excellent flammability through only one type of

flame retardants. Therefore, finding synergistic system is another way to improve flammability of polymers.

Many synergistic flame-retardant systems have been investigated, such as organic–inorganic, organic–organic, and inorganic–inorganic systems. Among all, phosphorus–silicon synergism has been reported and shown efficient synergism in polyurethane<sup>6</sup> and epoxy resin.<sup>7–10</sup> Hsiue et al.<sup>7</sup> prepared epoxy resin with phosphorus–silicon, and they found that a high limited oxygen index (LOI) value of 41 was obtained with a composition of phosphorus epoxides and organic siloxane diamines. Liu and Chou<sup>9</sup> studied the silicon sources of flame retardants, focusing on the flame-retardant mechanism of phosphorus–silicon synergism in the epoxy resins. The silicon compounds show significant effects on enhancing the thermal stability and char yield of epoxy resins. Recently, nano-SiO<sub>2</sub> and organic phosphorus show synergic effect in some polymer matrix. For example, Wang et al.<sup>11</sup> reported flame-retardant coatings with acrylic polymers, ammonium polyphosphate dipentaerythritol melamine (APP-DPER-MEL), and nano-SiO<sub>2</sub>. Better fire protection properties of coatings were obtained for the acrylic nanocomposites than those with

Correspondence to: J. Li (lijuan@nimte.ac.cn).

Contract grant sponsor: Program for Ningbo Innovative Research Team; contract grant number: 2009B21008.

Contract grant sponsor: Ningbo Natural Science Foundation of China; contract grant numbers: 2008A610063, 2010B22061.

conventional acrylic resins. Wu and Ke<sup>12</sup> prepared PET/PS/SiO<sub>2</sub> nanocomposite films and investigated their water absorption and thermal stable behaviors. They found that nano-SiO<sub>2</sub> in PET formed a barrier to both water and oxygen and may delay the degradation of PET in heating process.

The flammability of polymer is relevant to their behaviors of thermo-oxidative degradation at high temperature. Polymers will undergo thermal degradation when subjected to sufficient heat flux. Flame retardants act either in the condensed phase by changing the process of the pyrolytic decomposition or in the gas phase by scavenging carrier species, which are required during oxidation of volatile pyrolysis products in the flame. Wang and coworkers<sup>13–16</sup> systematically investigated the thermal oxidative degradation behavior of flame retardant PET composites at different heating rates in air using Kissinger and Flynn–Wall–Ozawa methods. These composites contained phosphorus groups, which are located in side chains or in main chains. The investigated flame retardants were [(6-oxide-6H-dibenz(c,e)(1,2) oxaphosphorin-6-yl)-methyl]-butanedioic acid (DDP) and 2-carboxyethyl (phenylphosphinic) acid (CEPP). The montmorillonite was used as filler in their composites. They found that the presence of phosphorus side groups tend to decrease the activation energy of copolyester in air. The introduction of montmorillonite in copolyester increased the thermal stability of nanocomposites. However, few studies have been done about the synergistic influence of organic phosphorus and nano-SiO<sub>2</sub> in PET composites on the thermal degradation behavior. In our previous work,<sup>17,18</sup> PET/SiO<sub>2</sub> nanocomposites were prepared by directly polymerizing PET monomer dispersed with organic modified silica nanoparticles. The dispersion of SiO<sub>2</sub> in PET, mechanical performance, crystallization, and melting behaviors of composites were investigated. In this article, nano-SiO<sub>2</sub> was used to assist DDP to improve the fire retardance of PET. The copolyesters PET-co-DDP, PET/SiO<sub>2</sub>, and PET-co-DDP/SiO<sub>2</sub> were prepared by *in situ* polymerization. The dispersion of nano-SiO<sub>2</sub> in PET was observed with transmission electron microscope (TEM) and scanning electron microscope (SEM). The effect of phosphorus and silicon on thermal degradation of PET was investigated with thermogravimetric analysis (TGA). Thermal degradation kinetics was determined using the Kissinger and Flynn–Wall–Ozawa methods.

## EXPERIMENTAL

### Materials

Terephthalic acid (TPA) and ethylene glycol (EG) were supplied by Changzhou Huayuan Radics Co.

**TABLE I**  
Summary of Nanoparticle Characteristics

Analysis	Results
Weight percent of silica (wt %)	30
Particle size (nm)	~12
Density (g/cm <sup>3</sup> )	1.2
PH value	10

(Jiangsu, China). DDP was provided by Mingshan Fine Chemical Industry Co. (Shandong, China). Sb<sub>2</sub>O<sub>3</sub> and triphenyl Phosphite were offered by H.V. Chemical Co. and China National Medicines Co., respectively. The aqueous solution of nano-SiO<sub>2</sub> was purchased from Zhoushan Mingri Nano-Company (Zhejiang, China). Parameters of the aqueous solution of SiO<sub>2</sub> nanoparticles were summarized in Table I (data from the manufacturer). The sample contains 30 wt % SiO<sub>2</sub> and about 70 wt % water.

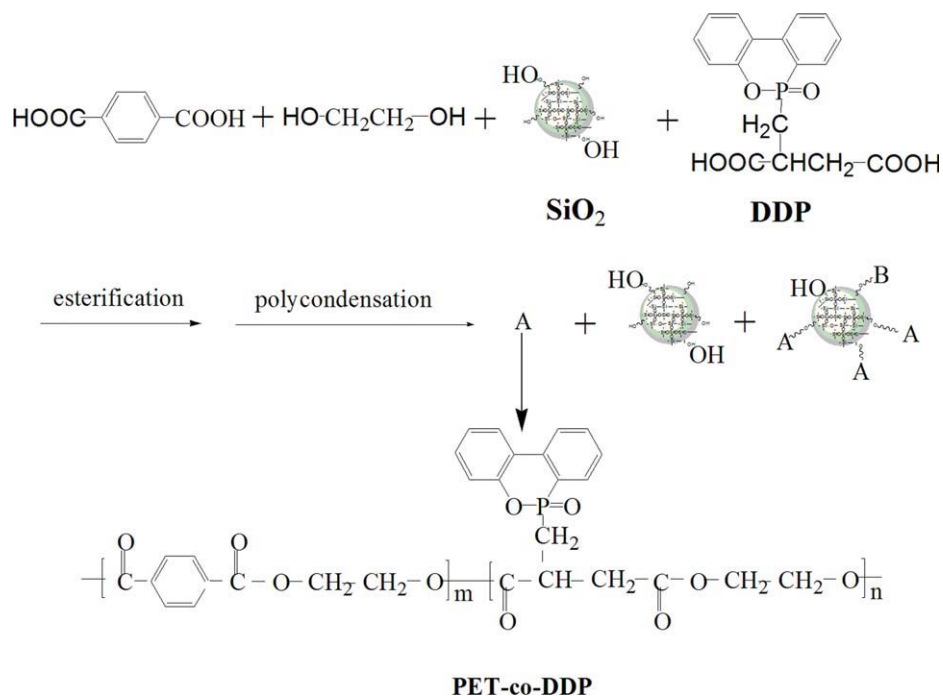
### Preparation of PET nanocomposites

All the copolyesters were synthesized through *in situ* polycondensation in a 1L reactor. This process was similar to the polymerization of PET nanocomposites in our previous work<sup>17,18</sup>, which is shown in Scheme 1 as follows:

The samples were fabricated and named as PET, PET1, PET2, PET3, and PET4, respectively, in which PET, PET1, and PET2 are corresponding to PET, PET/SiO<sub>2</sub> nanocomposites, and PET-co-DDP copolyester, respectively, and PET3 and PET4 are PET-co-DDP/SiO<sub>2</sub> nanocomposites with different SiO<sub>2</sub> contents. Table II shows the composition, intrinsic viscosities (IVs), and LOI values of different copolyesters. It can be seen that the LOI value increases to different extent when element Si or P or both were introduced into the PET. A LOI value of 33 could be obtained in PET4 when 2 wt % SiO<sub>2</sub> and 5 wt % DDP were added. Considering the LOI value of PET2, PET3, and PET4 together, it can be found a synergistic effect in LOI happened when the ratio of DDP to SiO<sub>2</sub> is 5 : 2. It indicates that the synergistic effect between DDP and SiO<sub>2</sub> happens when there is an appropriate ratio of DDP to SiO<sub>2</sub>. Specific synergistic mechanism will be studied in detail in the following work.

### Characterization

The IVs of the copolyesters were measured using an Ubbelohde viscometer at 25°C in phenol/1, 1, 2, 2-tetrachloroethane (50/50, w/w) solution. The LOI value was determined according to GB/T2406-93. TEM observation was carried out using a JEOL100C-XIITEM. The specimens about 80–100 nm for TEM



**Scheme 1** Reaction route of PET copolyester. [Color figure can be viewed in the online issue, which is available at [wileyonlinelibrary.com](http://wileyonlinelibrary.com).]

observation were prepared using Ultracut Uct at  $-80^{\circ}\text{C}$ . HITANCHI S4800 was used to carry out SEM observation. The samples were gilded on a HITANCHI 1045 instrument. The TGA was performed by using a SDT Q600 instrument. The experiments were conducted in nitrogen and air. Various heating rates of  $10^{\circ}\text{C}/\text{min}$ ,  $20^{\circ}\text{C}/\text{min}$ ,  $30^{\circ}\text{C}/\text{min}$ , and  $40^{\circ}\text{C}/\text{min}$  were taken to calculated kinetics of thermal degradation.

## RESULTS AND DISCUSSION

### Dispersion of nano-SiO<sub>2</sub>

It is known that the properties of the composites are significantly affected by the dispersion of the fillers in it. Figure 1 shows the TEM morphology of copolyesters PET1 and PET3. The dark particles are the SiO<sub>2</sub> particles. It is found that in PET1, the size of the SiO<sub>2</sub> conglomeration is smaller than 60 nm, and the SiO<sub>2</sub> nanoparticles are dispersed uniformly in the copolyester. Addition of DDP has slightly effect on the dispersion of SiO<sub>2</sub> in polymer, as shown in Figure 1(b), which is attributed to the compatibility of aqueous solution of SiO<sub>2</sub> and EG that they mixed uniformly with each other. So, a good dispersion of silica in the polymer matrix was obtained after polymerization.

SEM was also used to observe the dispersion of SiO<sub>2</sub> nanoparticles in the composites. The SEM morphology of copolyesters PET1 and PET3 is shown in Figure 2. In the SEM images, the white dots repre-

sent SiO<sub>2</sub>. It can be seen that the dispersion of SiO<sub>2</sub> nanoparticles in copolyesters is uniform, which is in accordance with the TEM results.

### TG analysis in nitrogen

TG and DTG curves of the samples in nitrogen are shown in Figure 3(a,b), respectively. One-step decomposition is found for all samples. The decomposition temperature  $T_{d(1\%)}$ ,  $T_{d(5\%)}$ , and  $T_{d(10\%)}$  at which there is 1%, 5%, and 10% of weight loss, respectively, and the maximum decomposition rate temperature ( $T_{\text{max}}$ ) for all samples were determined from Figure 3 and summarized in Table III. It is found that the  $T_{d(1\%)}$  for PET2 and PET3 is  $6.2^{\circ}\text{C}$  and  $2.5^{\circ}\text{C}$  higher than PET, respectively, and PET4 and PET5 is  $1.6^{\circ}\text{C}$  and  $11.6^{\circ}\text{C}$  lower than PET, respectively. It indicates that the coexistence of DDP and SiO<sub>2</sub> results in the decrease of decomposition temperature at the early stage and  $T_{d(1\%)}$  decreases

**TABLE II**  
Properties of Copolyesters

Samples	Composition			IV	LOI
	PET (wt %)	DDP (wt %)	SiO <sub>2</sub> (wt %)		
PET	100	0	0	0.72	24
PET1	98	0	2	0.65	25
PET2	97	3	0	0.69	29
PET3	95	3	2	0.64	29
PET4	93	5	2	0.71	33

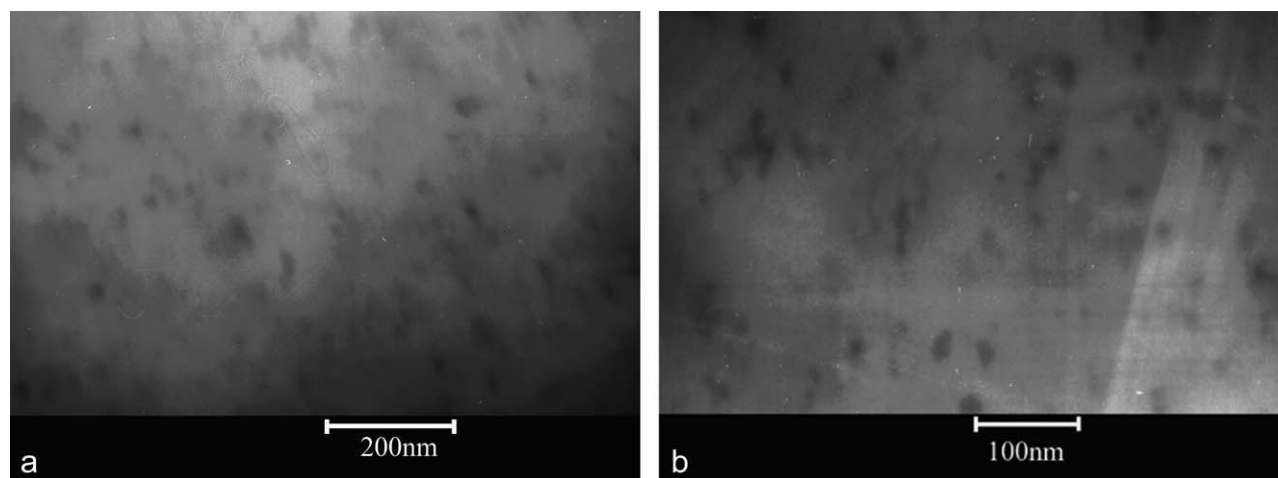


**Figure 1** TEM of copolyesters a) PET1 and b) PET3.

with the DDP content in PTT-*co*-DDP/SiO<sub>2</sub> nanocomposites. With the development of decomposition, the highest  $T_{\max}$  value is obtained for PET-*co*-DDP. The results show that the effect of SiO<sub>2</sub> and DDP on decomposition of copolyester is different. The residues at 600°C for different copolyester are shown in Table III. Obviously, the addition of SiO<sub>2</sub> increases the residues at 600°C of PET slightly; however, the existence of the DDP decreases the residues at 600°C of PET. In the PET-*co*-DDP/SiO<sub>2</sub>, the residue at 600°C is higher than PET and PET/SiO<sub>2</sub>. The SiO<sub>2</sub> and DDP show synergic effect on the residue at 600°C. With the increasing of DDP content, the residue at 600°C decreases.

Kissinger method was employed to calculate the activation energies of degradation as shown in Figure 4. The values of  $E_a$  are given in Table III. It can be seen that the existence of the DDP decreases the activation energy of the copolyester; however, the incorporation of SiO<sub>2</sub> tends to improve the activation energy of the composites. The activation energy of

PET3 is between PET1 and PET2, because of the opposite effects of SiO<sub>2</sub> and DDP on activation energy. With the increasing of DDP content, the value of activation energy for PET-*co*-DDP/SiO<sub>2</sub> improves. The decomposition process is complicated, and the introduction of SiO<sub>2</sub> changes the degradation behavior of copolyesters in nitrogen slightly.

#### TG analysis in air

Thermal degradation in air atmosphere is close to real flame condition. Figure 5 shows the TG and DTG curves of PET, PET1, PET2, PET3, and PET4 in air. Two-step decomposition is found for all samples in air. The detailed data of  $T_{d(1\%)}$ ,  $T_{d(5\%)}$ ,  $T_{d(10\%)}$ ,  $T_{\max 1}$ , and  $T_{\max 2}$  are shown in Table IV. Obviously, the existence of DDP and SiO<sub>2</sub> has great effect on the temperature at the early decomposition. The temperature for all composite samples at 1-wt % weight loss shifts to higher temperature. The  $T_{d(1\%)}$  for PET/SiO<sub>2</sub> and PET-*co*-DDP is about 30°C and 16°C higher than

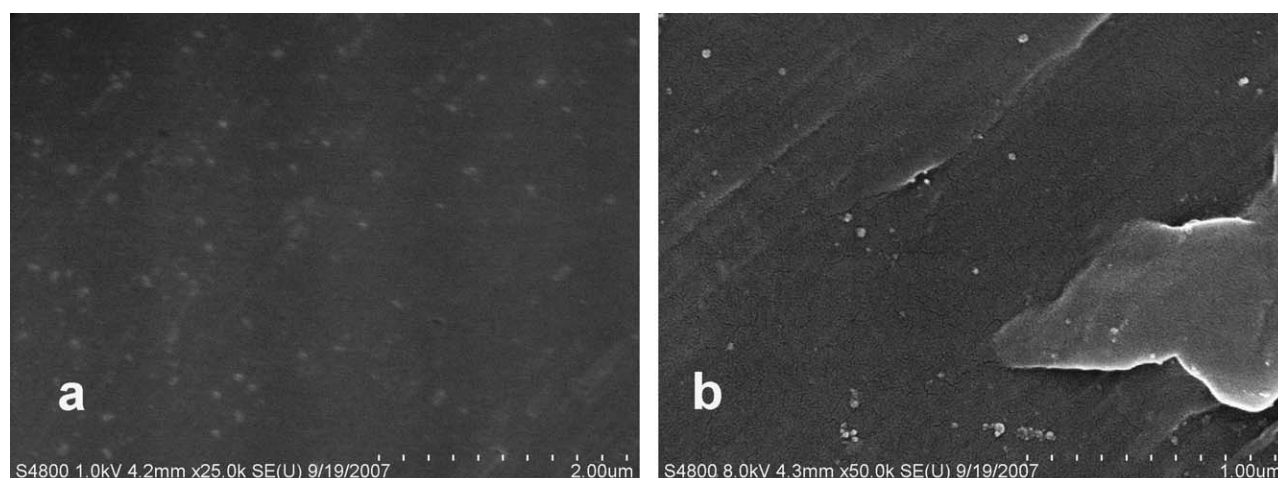


**Figure 2** SEM of copolyesters a) PET1 and b) PET3.

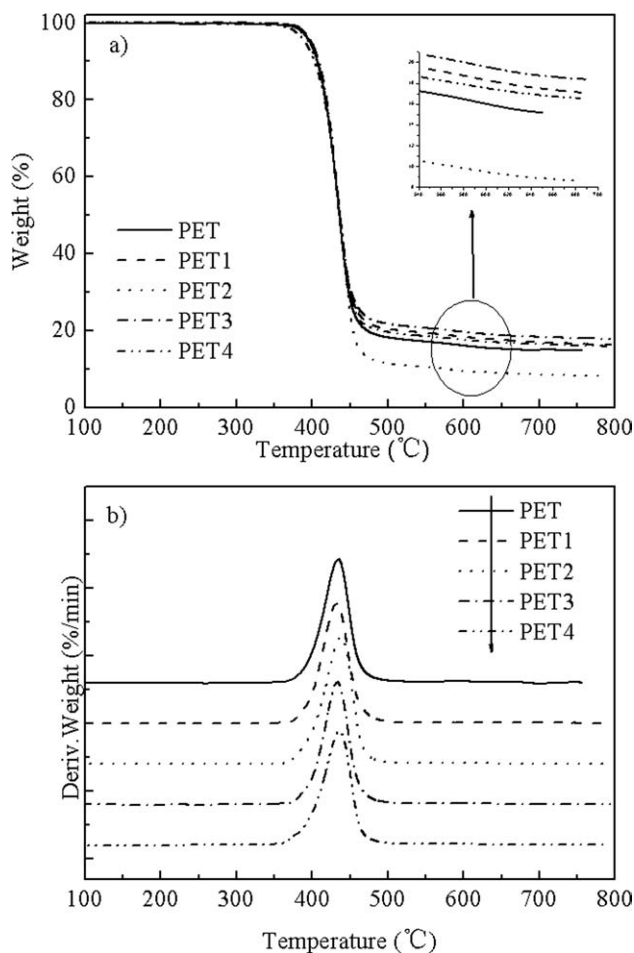


**Figure 3** TG and DTG curves of various copolyesters in nitrogen at heating rate of 10°C/min.

PET, respectively, and that for PET3 is 40°C higher than PET. With the development of decomposition, the effect of SiO<sub>2</sub> and DDP on degradation temperature is weakened. The  $T_{max1}$  and  $T_{max2}$  improve slightly for all PET composites. The results suggest that the SiO<sub>2</sub> and DDP enhance the thermal stability of PET in air greatly. The residues at 600°C for different copolyester are shown in Table IV. The residue at 600°C of PET/SiO<sub>2</sub> is 1.8 times higher than that for PET after deducting the 2 wt % SiO<sub>2</sub>. The existence

**TABLE III**  
Thermal Properties and Activation Energies of Copolyesters in Nitrogen Determined by Kissinger Method

Samples	PET	PET1	PET2	PET3	PET4
$T_{d(1\%)}(°C)$	375.7	381.9	378.2	374.1	364.1
$T_{d(5\%)}(°C)$	397.4	398.7	395.2	398.3	391.0
$T_{d(10\%)}(°C)$	407.0	408.0	405.4	408.3	403.3
$T_{max}(°C)$	435.4	433.5	438.6	434.5	437.0
Residues at 600°C (%)	16.0	18.3	9.5	19.7	17.4
$E_a(kJ/mol)$	157.1	176.3	156.1	170.8	178.0
R	0.9987	0.9989	0.9985	0.9995	0.9996

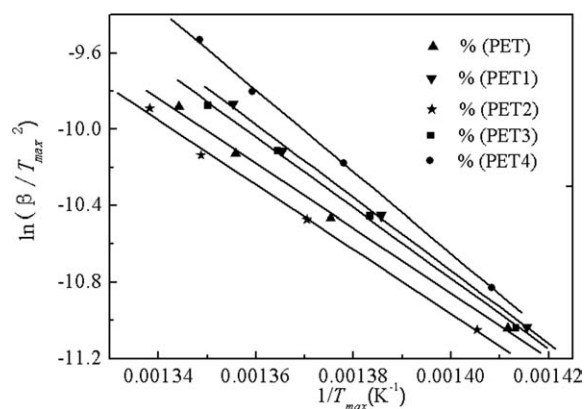


**Figure 4** Kissinger method applied to TG data of various copolyesters at different heating rates in nitrogen.

of DDP also increases the residues at 600°C of PET slightly. However, in the PET-co-DDP/SiO<sub>2</sub> composite, the residue at 600°C is about 2.7 times higher than PET and PET/SiO<sub>2</sub>, indicating good synergic effect between SiO<sub>2</sub> and DDP. With the increasing of DDP content, the residue increases. According to the barrier model,<sup>19</sup> nano-SiO<sub>2</sub> may move to the surface

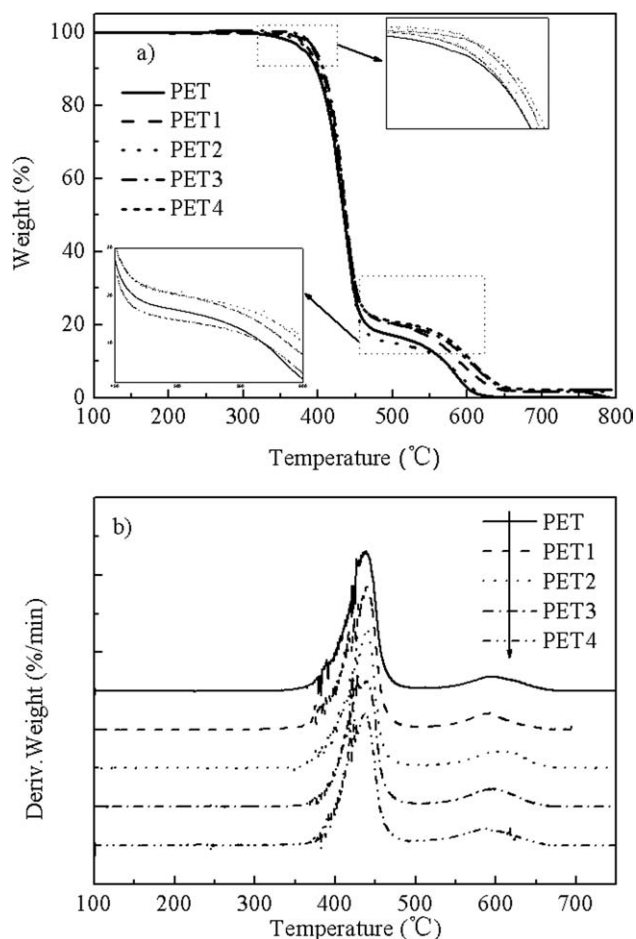


**Figure 5** TG and DTG curves of various copolyesters in air at heating rate of 10°C/min.

**TABLE IV**  
**Thermal Properties and Activation Energies of**  
**Copolyesters in Air Determined by Kissinger Method**

Samples	PET	PET1	PET2	PET3	PET4
$T_{d(1\%)}(^{\circ}\text{C})$	338.8	368.6	354.6	378.6	368.2
$T_{d(5\%)}(^{\circ}\text{C})$	381.8	393.9	386.4	393.3	388.8
$T_{d(10\%)}(^{\circ}\text{C})$	397.5	404.7	398.6	406.9	401.1
$T_{\text{max}1}(^{\circ}\text{C})$	438.8	437.1	439.5	435.2	439.3
$T_{\text{max}2}(^{\circ}\text{C})$	584.2	586.5	592.6	599.5	613.6
Residue at 600°C (wt %)	2.7	7.8	3.7	10.2	11.2
$E_a$ (kJ/mol)	188.4	202.3	169.8	169.3	184.1
R	0.9939	0.9989	0.9146	0.9949	0.9954

to form a crosslink barrier, thus prevent the diffusion of gaseous decomposition products and also act as a heat insulation layer. Therefore, better thermal stability and higher charring residue is obtained for PET composites than PET.

The TG curves of PET, PET1, PET2, PET3, and PET4 in air at different heating rates of 10, 20, 30, and 40°C/min are shown in Figure 6. The fitting straight lines determined by Kissinger method are shown in Figure 7, and the activation energies for all samples are listed in Table IV. It can be seen that introduction of SiO<sub>2</sub> increases the degradation activation energy of the PET composites; the values for PET and PET/SiO<sub>2</sub> are 188.4 and 202.3 kJ/mol,

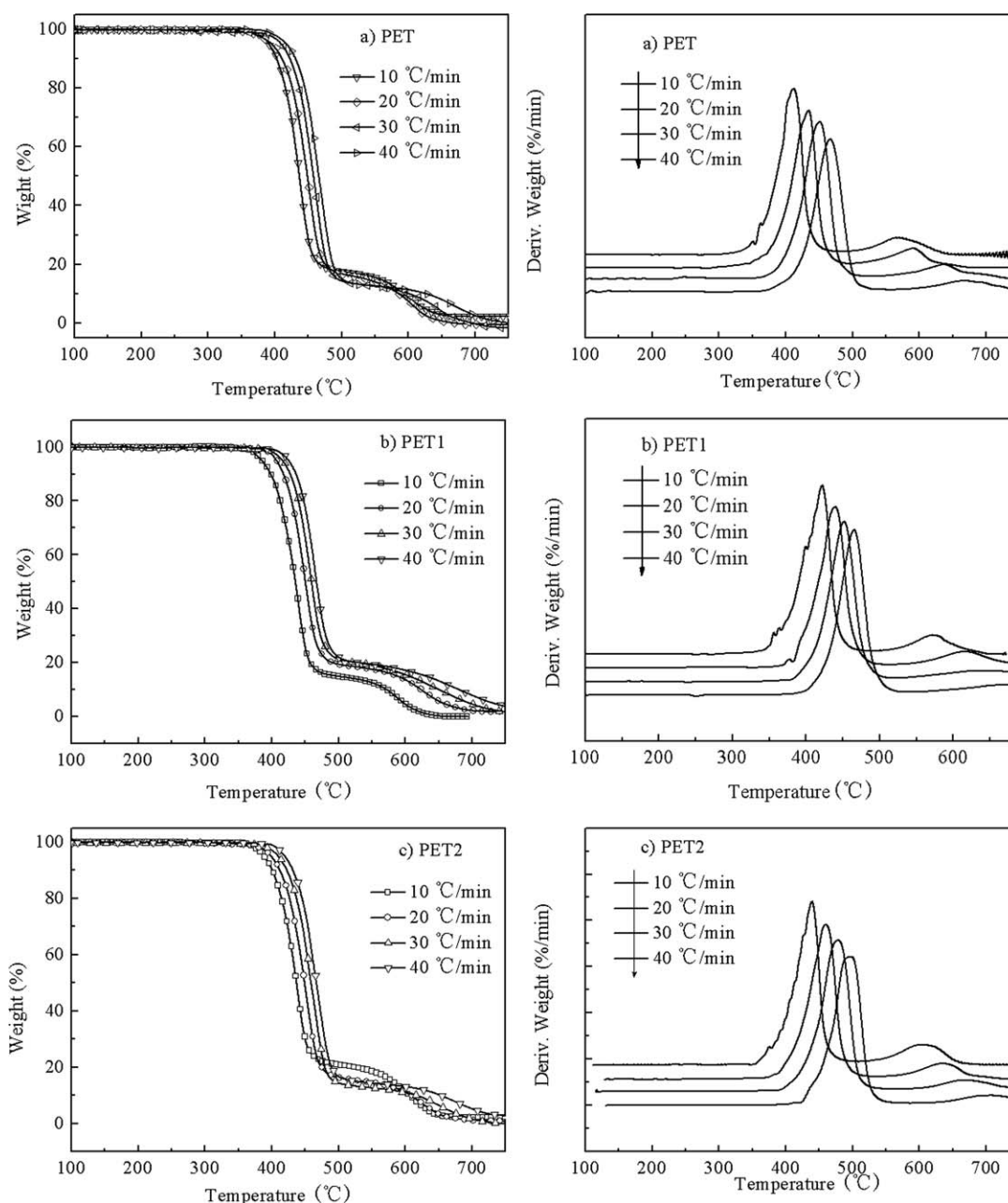


**Figure 6** TG and DTG curves of different copolyesters in air at different heating rates a) PET and b–e) PET1–4.

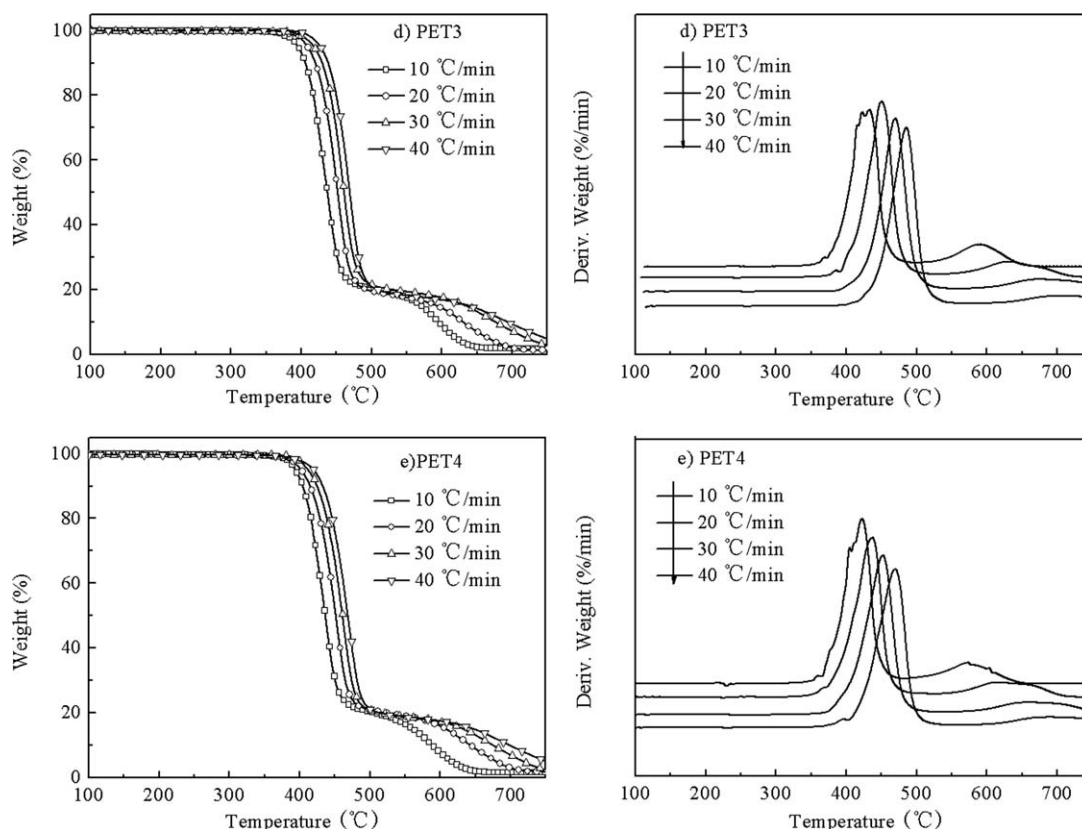


Figure 6 (Continued)

respectively. However, the incorporation of DDP decreases the degradation activation energy for the copolyester in air, which is in accordance with the reports of Wang and coworkers.<sup>13–16</sup> In the PET-*co*-DDP/SiO<sub>2</sub>, the activation energy for PET3 remains almost the same value as PET2. With the DDP content increasing, the activation energy for PET4 is improved. The higher apparent activation energy of thermal oxidative degradation is ascribed to the better thermal stability of the charring layer with good quality formed in the burning process. In addition, the apparent activation energy values are found to be higher in air than in nitrogen. Probably, nano-SiO<sub>2</sub> in PET plays a strong barrier to both water and oxygen and thus delays the degradation of PET in heating processing in air.<sup>12</sup>

Kinetic information of the thermal degradation of polymers can be extracted from dynamic experiments by various methods. However, all kinetic studies assume that the isothermal rate of conversion,  $d\alpha/dt$ , is a linear function of a temperature-dependent rate constant,  $k$ , and a temperature-independent function of the conversion,  $f(\alpha)$ , that is:

$$\frac{d\alpha}{dt} = kf(\alpha), \quad (1)$$

where  $f(\alpha)$  and  $k$  are functions of conversion and temperature in Eq. (1), respectively.

According to Arrhenius,

$$k = Ae^{-E/RT}, \quad (2)$$

where  $E$  is the activation energy,  $A$  is the pre-exponential factor, and  $R$  is the gas constant.  $f(\alpha)$  depends on the particular decomposition mechanism. Substitution of Eq. (2) in Eq. (1) gives:

$$\frac{d\alpha}{dt} = Af(\alpha)e^{-E/RT}. \quad (3)$$

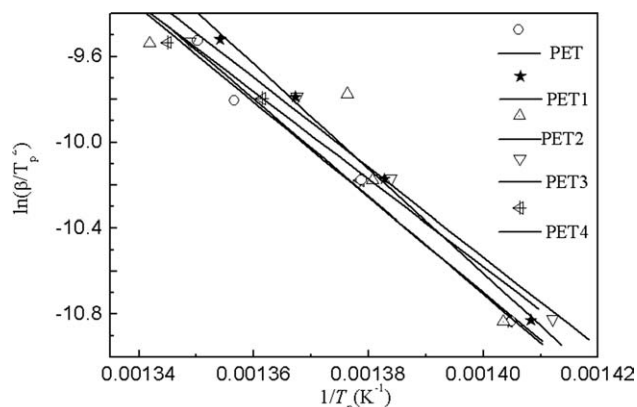


Figure 7 Kissinger method applied to TG data of various copolyesters at different heating rates in air.

We assume the heating rate of the sample temperature,  $\beta = dT/dt$ , is constant, and the variation in the degree of conversion can be analyzed as a function of temperature depending on the time of heating. Therefore, the reaction rate can be rewritten as follows:

$$\frac{d\alpha}{dt} = \frac{d\alpha}{dT} \frac{dT}{dt} = \beta \frac{d\alpha}{dT}. \quad (4)$$

A combination of eqs. (3) and (4) leads to

$$\frac{d\alpha}{dT} = \frac{A}{\beta} e^{-\frac{E}{RT}} f(\alpha) \quad (5)$$

$$\frac{1}{f(\alpha)} d\alpha = \frac{A}{\beta} e^{-\frac{E}{RT}} dT. \quad (6)$$

Integral of both two sides of Eq. (6), the left side from  $\alpha_0$ , the initial conversion rate, to  $\alpha_p$ , the conversion rate of the peak temperature, and the right side from  $T_0$ , the initial temperature, to  $T_p$ , the peak temperature, respectively, gives Eq. (7)

$$\int_{\alpha_0}^{\alpha_p} \frac{d\alpha}{f(\alpha)} = \frac{A}{\beta} \int_{T_0}^{T_p} e^{-\frac{E}{RT}} dT. \quad (7)$$

It can be assumed reasonably that  $\alpha_0 = 0$  when  $T_0$  is low and no reaction between 0 and  $T_0$ , so

$$\int_0^{\alpha_p} \frac{d\alpha}{f(\alpha)} = \frac{A}{\beta} \int_0^{T_p} e^{-\frac{E}{RT}} dT. \quad (8)$$

Usually, the simplest and most frequently used model for  $f(\alpha)$  in the analysis of TG data is

$$f(\alpha) = (1 - \alpha)^n, \quad (9)$$

where  $n$  is the order of the reaction.

Combination of eqs. (3) and (9) gives:

$$\frac{d\alpha}{dt} = A(1 - \alpha)^n e^{-E/RT}. \quad (10)$$

Kissinger method

Kissinger method<sup>20</sup> involves obtaining the temperature values  $T_{\max}$  that occurs at the maximum conversion rate, where  $d(da/dt)/dt$  is zero, differentiation of Eq. (10) with respect to  $t$  and setting the resulting expression to zero gives

$$\frac{E\beta}{RT_{\max}^2} = An(1 - \alpha_{\max})^{n-1} e^{-E/RT_{\max}}, \quad (11)$$

logarithm of both two sides of Eq. (11) gives

$$\ln\left(\frac{\beta}{T_{\max}^2}\right) = \left\{ \ln \frac{AR}{E} + \ln [n(1 - \alpha_{\max})^{n-1}] \right\} - \frac{E}{RT_{\max}} \quad (12)$$

Then, the activation energy can be investigated from the plots of  $\ln(\beta/(T_{\max})^2)$  versus  $1/T_{\max}$  at the maximum reaction rate, while the heating rate of the experiments is kept constant, even if no precise knowledge of the reaction mechanism known.

Flynn–Wall–Ozawa method

Flynn–Wall–Ozawa method<sup>21,22</sup> method, which is essentially the same as that of Flynn and Wall, represents a relatively simple method of determining activation energy directly from plots of weight loss versus temperature data obtained at several heating rates. Equation (7) is integrated using Doyle's<sup>23</sup> approximation, the result of the integration after taking logarithms is

$$\log f(\alpha) = \log \frac{AE}{R} - \log \beta - 2.315 - 0.4567 \frac{E}{RT} \quad (13)$$

$$\log \beta = \left[ \log \frac{AE}{R} - \log f(\alpha) - 2.315 \right] - 0.4567 \frac{E}{RT}, \quad (14)$$

where  $b$ ,  $A$ ,  $E$ , and  $T$  have the known meanings, and  $f(\alpha)$  is the integral function of conversion. Flynn–Wall–Ozawa method is one of the integral methods that can determine the activation energy without the knowledge of reaction order. It is used to determine the activation energy for given values of conversion. The activation energy for different conversion values can be calculated from plots of  $\log \beta$  versus  $1/T$ .

It should be noted that the correlation coefficient of PET2's fitting straight lines is only 0.9146, which is indicating higher error. Thermal degradation is a complex multistage process: thermal oxidation, pyrolysis, and thermal hydrolysis. Take the degradation of PET for example; it first undergoes random scission of ester bonds that generates carboxyl end groups and vinyl ester, and such random scissions may lead to a complex degradation pathway such as crosslinking, small fragments from secondary reactions, and other complex chemical changes. Over the temperature range of 300–400°C, a highly cross-linked polyaromatic char intermediate has been formed in PET and then converts to volatile products or others. Several reactions happened during the generation of polyaromatic char, such as chain stripping and cyclization/crosslinking.<sup>24,25</sup> Thus, there must be wide variations in the calculated activation energy depending on different mathematical approach taken in the analysis. To get more applicable data, Flynn–Wall–Ozawa model is used to calculate the activation energy of copolyester. The difference between Flynn–Wall–Ozawa and Kissinger



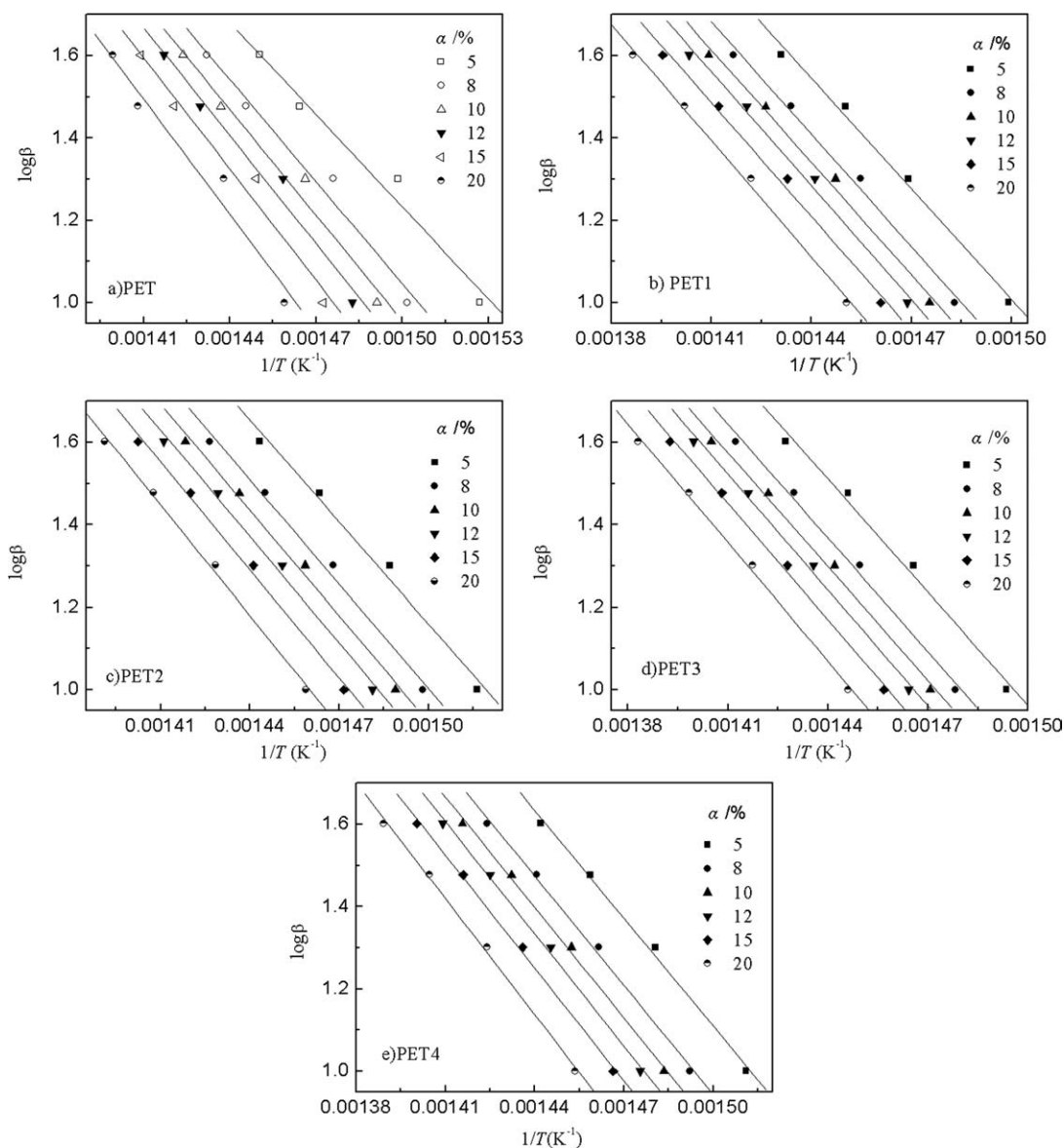


**Figure 8** Plots of  $\log\beta$  against  $1/T$  at conversion degree (a) 5%–20% for a) PET and b–e) PET1–4 in air.

methods is that the treatment of the TG data at the different heating rates and at the given conversion degree ( $\alpha$ ) are required. According to Eq. (14), the plot of  $\log\beta$  against  $1/T$  makes a fitted straight line. The slope of this straight line was used to calculate the activation energy of the involved system. If the straight lines fitted at different conversion degrees  $\alpha$  parallel each other, this method proves to be applicable to the investigated system. Because Flynn–Wall–Ozawa method uses Doyle approximation, the calculated values limited in the conversion degree range of 5%–20% are reliable.<sup>23</sup> The fitting straight lines at the conversion degree ranging from 5% to 20% are shown in Figure 8. It is found that the fitting straight lines are almost parallel, indicating the applicability of Ozawa method to our systems in the investigated conversion range.

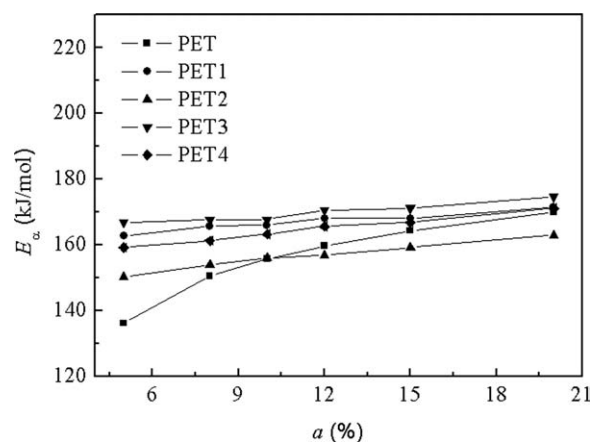


**Figure 9** Activation energies obtained by Flynn–Wall–Ozawa method versus conversion degree ( $\alpha$ ) for different samples.

TABLE V  
Activation Energies of Different Copolyesters in Air Determined by Flynn–Wall–Ozawa Method

Samples	$\alpha$ (%)	5	8	10	12	15	20	Mean kJ/mol
PET	$E_a$	136.1	150.4	155.7	159.6	164.3	169.9	153.0
	$r$	0.9883	0.9891	0.9891	0.9880	0.9879	0.9823	
PET1	$E_a$	162.8	165.7	166	168.1	168.1	171.4	167.1
	$r$	0.996	0.9961	0.9961	0.9957	0.9965	0.9980	
PET2	$E_a$	150.2	153.9	155.9	156.8	159.2	162.9	156.6
	$r$	0.9935	0.9957	0.9966	0.9967	0.9974	0.9983	
PET3	$E_a$	166.7	167.6	167.7	170.5	171.2	174.6	170.7
	$r$	0.9946	0.9964	0.997	0.9975	0.9983	0.9984	
PET4	$E_a$	159.2	161.2	163.2	165.6	166.8	171.1	165.2
	$r$	0.9979	0.9981	0.9986	0.9985	0.9989	0.9989	

From the slopes of the fitted straight lines of various samples at different conversion degrees (Fig. 8), the corresponding activation energy was calculated. Figure 9 shows the plots of the obtained activation energy  $E_a$  as a function of  $a$ . It can be seen that the  $E_a$  values for PET increase with increasing  $a$ , indicating that the thermal stability of PET is improved, and the thermo-oxidative degradation is not accelerated very quickly. This is different from that of polypropylene (PP),<sup>26</sup> which related with a better physical properties and more stable structure of PET than PP. For all copolyester samples,  $E_a$  changed slightly with increasing  $a$ . The average activation energies are shown in Table V. The values decrease according to the following order: PET3 > PET1 > PET4 > PET2 > PET, which is in accordance with the trend of the early decomposition temperature [ $T_{d(1\%)}$ ]. The introduction of SiO<sub>2</sub> increases the degradation activation energy of the composites, and the incorporation of DDP also increases the degradation activation energy for the copolyester in air. However, in the PET-*co*-DDP/SiO<sub>2</sub>, the activation energy for PET3 is higher than PET2. The activation energy for PET4 decreased with an increasing DDP content. The results are not in accordance with that obtained by Kissinger method. The possible reason can be the limitation of the conversion degree range of 5%–20% in Flynn–Wall–Ozawa method. While, the apparent activation energy by Kissinger method was obtained from the relationship between the  $\ln(\beta/(T_{\max})^2)$  and  $T_{\max}$ . Earlier results reflect the flame retardant role of SiO<sub>2</sub> and DDP in PET matrix. When PET copolyester is heated, the charring layers are induced by the SiO<sub>2</sub> and DDP. They cover on the underlying matrix and prevent the PET matrix from further decomposition, hence leading to the increase of activation energy of thermal decomposition of the copolyester.

## CONCLUSIONS

The phosphorus-containing copolyester (PET-*co*-DDP)/SiO<sub>2</sub> nanocomposites were synthesized by

*in situ* polymerization of TPA, EG, DDP, and SiO<sub>2</sub> nanoparticles. The SiO<sub>2</sub> was dispersed in the copolyesters uniformly. Thermal degradation behaviors of PET, PET/SiO<sub>2</sub>, PET-*co*-DDP, and PET-*co*-DDP/SiO<sub>2</sub> in nitrogen and air were investigated by TG analysis, and the kinetics were calculated with Kissinger and Flynn–Wall–Ozawa methods. The introduction of SiO<sub>2</sub> increases the activation energy of PET while that for PET-*co*-DDP is decreased whether in nitrogen or air ambience. The coexistence of SiO<sub>2</sub> and DDP has better synergic effects on the early decomposition and the late residue in air. In the PET-*co*-DDP/SiO<sub>2</sub> system, the activation energy increases when the DDP content increases. However, at the conversion degree from 5% to 20% opposite results are obtained. The effect of SiO<sub>2</sub> and DDP on the thermal degradation of PET is lower in nitrogen than air.

## References

- Wang, Y. Z. Flame retarding design for polyester fibers. Chengdu: Sichuan Science and Technology Press, 1994.
- Wang, Y. Z.; Chen, X. T.; Tang, X. D. *J Appl Polym Sci* 2002, 86, 1278.
- Wang, D. Y.; Ge, X. G.; Wang, Y. Z.; Wang, C.; Qu, M. H. *Macromol Mater Eng* 2006, 291, 638.
- Deng, Y.; Zhao, C. S.; Wang, Y. Z. *Polym Degrad Stab* 2008, 93, 2066.
- Wang, C. S.; Lin, C. H. *Polymer* 1999, 40, 747.
- Cai, Y. Y.; Fan, H.; Chen, H. *Thermosetting Resin* 2007, 22, 50.
- Hsiue, G. H.; Tsaio, I.; Liu, Y. L. *J Appl Polym Sci* 2000, 78, 1.
- Mercado, L. A.; Galià, M.; Reina, J. A. *Polym Degrad Stab* 2006, 91, 2588.
- Liu, Y. L.; Chou, C. I. *Polym Degrad Stab* 2005, 90, 515.
- Spontón, M.; Mercado, L. A.; Ronda, J. C.; Galià, M.; Cádiz, V. *Polym Degrad Stab* 2008, 2025, 93.
- Wang, Z. Y.; Han, E. H.; Ke, W. *Polym Degrad Stab* 1937 2006, 91.
- Wu, T. B.; Ke, Y. C. *Polym Degrad Stab* 2006, 91, 2205.
- Wu, B.; Wang, Y. Z.; Wang, X. L.; Yang, K. K.; Jin, Y. D.; Zhao, H. *Polym Degrad Stab* 2002, 76, 401.
- Zhao, H.; Wang, Y. Z.; Wang, D. Y.; Wu, B.; Chen, D. Q.; Wang, X. L.; Yang, K. K. *Polym Degrad Stab* 2003, 80, 135.
- Wang, D. Y.; Wang, Y. Z.; Wang, J. S.; Chen, D. Q.; Zhou, Q.; Yang, B.; Li, W. Y. *Polym Degrad Stab* 2005, 87, 171.

16. Ge, X. G.; Wang, D. Y.; Wang, C.; Qu, M. H.; Wang, J. S.; Zhao, C. S.; Jing, X. K.; Wang, Y. Z. *Eur Polym Mater* 2007, 43, 2882.
17. Tian, X. Y.; Zhang, X.; Liu, W. T.; Zheng, J.; Ruan, C. J.; Cui, P. *J Macromol Sci Part B: Phys* 2006, 45, 507.
18. Liu, W. T.; Tian, X. Y.; Cui, P.; Li, Y.; Zheng, K.; Yang, Y. *J Appl Polym Sci* 2004, 91, 1229.
19. Vyazovkin, S.; Dranca, I.; Fan, X. W.; Advincola, R. *Macromol Rapid Commun* 2004, 25, 498.
20. Kissinger, H. E. *Anal Chem* 1957, 29, 1702.
21. Ozawa, T. *Bull Chem Soc Jpn* 1965, 38, 1881.
22. Flynn, J. H.; Wall, L. A. *J Res Natl Bur Stand Sec A: Phys Chem* 1966, 70, 487.
23. Doyle, C. D. *Nature* 1965, 207, 290.
24. Thitivat, S. *Basic Chemistry of Flame Retardation of Poly (ethylene terephthalate)*; Dissertations, Marquette University, 1987.
25. Zimmerman, H.; Nguyen, T. K. *Polym Eng Sci* 1980, 20, 680.
26. Chen, Y. H.; Wang, Q. *Polym Degrad Stab* 2007, 92, 280.